Synthesis and Characterization of Poly(acrylic acid-*co*-*N*-[3-(dimethylamino)propyl]-methacrylamide) Hydrogel Membranes for Biomedical Applications

Anup Das,[1,2] Alok R. Ray[1,2]

[1]*Centre for Biomedical Engineering, Indian Institute of Technology Delhi, New Delhi 110016, India*
[2]*Biomedical Engineering Unit, All India Institute of Medical Sciences, New Delhi 110029, India*

Received 14 October 2007; accepted 14 November 2007
DOI 10.1002/app.27665
Published online 23 January 2008 in Wiley InterScience (www.interscience.wiley.com).

ABSTRACT: A series of new hydrogel membranes with different compositions of acrylic acid (AAc) and *N*-[3-(dimethylamino)propyl]-methacrylamide (DMAPMA) were prepared by aqueous copolymerization, without using chemical crosslinker or radiation. Chemical structure of the membranes (PADMAs) was characterized by Fourier transform infrared spectroscopy (FTIR). Swelling experiments were carried out in simulated body fluid (SBF) at 37 ± 1°C to investigate degree of swelling, dimensional stability, and pore size of the PADMA membranes. In SBF, the variation of pore size with membrane composition was monitored by optical microscopic technique. Morphology of the membranes was characterized, before and after exposure to SBF, by scanning electron microscopy (SEM). It was observed that the membranes are composed of closely packed nanogels of ~200 nm. Macroporous network structure of the SBF-swollen PADMA was also observed to be composed of interconnected nanogels. Blood compatibility of the PADMA membranes was evaluated *in vitro*, by performing hemolysis assay and thrombogenicity assay. The extent of hemolysis due to PADMA membranes was found to be <2%, which ensured that all of the membranes were highly hemocompatible. Salicylic acid (SA) was chosen as a model drug. Diffusion coefficient of SA through PADMA membranes was investigated. It was observed that membrane composition regulates both pore size and drug diffusion. © 2008 Wiley Periodicals, Inc. J Appl Polym Sci 108: 1273–1280, 2008

Key words: acrylic acid; diffusion; hemocompatible; hydrogels; membranes

INTRODUCTION

Hydrogels have received significant attention in diversified fields because of their promising applications, such as drug delivery,[1–3] bioseparations,[4,5] immobilization of enzymes and cells,[6–8] biosensors,[9,10] and making artificial muscles.[11–13] These are three-dimensional networks of hydrophilic polymers. The network structure in hydrogels allows imbibing and retaining large amount of water and biological fluids but prevents the dissolution of polymer chains/segments.

Various chemical and physical crosslinking methods are in use to design hydrogels.[14] Each method brings with it its own benefits and limitations depending on the desired use and application of the gels. The disadvantages of chemically crosslinked gels include the difficulty of their processing, the presence of significant solvent fraction, and their low biocompatibility.[15] To overcome these limitations, physical crosslinking methods are becoming more and more promising. The conventional physical gels have been formed in associating one or several complementary polymers by ionic or hydrophobic interactions, hydrogen bonding, physical entanglement, or a combination of several of these interactions.[16–18] It was reported that monolithic hydrogel matrices could be fabricated by simply mixing two oppositely charged polymers as well as by copolymerization of oppositely charged monomers.[19,20] Long-range Coulombic attraction was shown to be responsible for physical crosslinking.

The aim of our present work was to develop physically crosslinked hydrogels, which are stable in physiological fluid. Anionic monomer acrylic acid (AAc) was copolymerized with cationic monomer *N*-[3-(dimethylamino)propyl]-methacrylamide (DMAPMA) in aqueous medium. As far as we know, P(AAc-*co*-DMAPMA) copolymer has not been reported so far in any hydrogel formulation. Long-range Coulombic interaction was anticipated between AAc and DMAPMA units in the resulting copolymers. A series of five P(AAc-*co*-DMAPMA) membranes (PADMAs) were successfully fabricated at 41 ± 1°C. It is worthwhile to mention here that AAc has long been used to design hydrogels for various applications.[21–24] However, DMAPMA has started receiving attention to design skin care

Correspondence to: A. R. Ray (alokray@cbme.iitd.ernet.in).

Journal of Applied Polymer Science, Vol. 108, 1273–1280 (2008)

cosmetics, anti microbial polymers, temperature sensitive polymers, protein estimation, protein separation, etc.[25–29] In this contribution, PADMA membranes were evaluated as monolithic hydrogel matrices to be used in contact of physiological fluid and blood. Degree of swelling is one of the most important parameters which govern various important properties of hydrogels like hydrodynamic volume and diffusion coefficient. Again, degree of swelling itself depends on various external stimuli, such as pH, ionic strength, and temperature. To imitate the behavior of PADMA membranes in contact of physiological fluid, a series of *in vitro* experiments were conducted in simulated body fluid (SBF) at 37 ± 1°C. Important properties/parameters such as dimensional stability, degree of swelling, pore size, and morphology were examined. Thrombus formation and rupture of red blood cell (RBC) are two major concerns in the blood compatibility of a material.[30] Thrombus formation and RBC rupture due to PADMA membranes were evaluated by thrombogenicity assay and hemolysis assay, respectively. Diffusion experiments were carried out with PADMA membranes, taking salicylic acid (SA) as a model drug.

EXPERIMENTAL

Materials

Acrylic acid (AAc; G.S. Chemicals, India) was distilled under vacuum before use. *N*-3-[(dimethylamino) propyl]-methacrylamide (DMAPMA; Aldrich, USA) was used as received. Ammonium persulphate (APS; Qualigens Fine Chemicals, India), 2-butanone (Qualigens Fine Chemicals, India), *N*,*N*,*N*′,*N*′-tetramethyl ethylene diamine (TEMED; SRL Pvt. Ltd, India), and salicylic acid (SA; Loba Chemic, India) were used without further purification. Simulated body fluid (SBF) was prepared according to Kokubo et al.,[31] by dissolving appropriate amounts of NaCl, $NaHCO_3$, KCl, $K_2HPO_4{\cdot}3H_2O$, $MgCl_2{\cdot}6H_2O$, $CaCl_2$, and Na_2SO_4 in distilled water and buffering to pH 7.4 at 37°C with tris(hydroxymethyl)aminomethane and 1*M* HCl solution.

Synthesis of PADMA membranes

PADMA membranes of five different monomer feed compositions were prepared by free radical aqueous copolymerization of AAc and DMAPMA, using APS and TEMED as the initiator and accelerator, respectively. The reactions were carried out in two steps and are shown in Scheme 1.

Prior to the reactions, five different monomer mixtures were prepared by controlled addition of DMAPMA to AAc with simultaneous stirring over a magnetic stirrer. Predetermined amount of water was then added to each of the monomer mixtures. The first step of the reactions was carried out at 27 ± 1°C in 100-mL three-neck round-bottom flask, equipped with a magnetic stir bar and a nitrogen line. Nitrogen gas was purged for 15 min, followed by the addition of TEMED (3.0 mol %) and conc. aqueous solution of APS (0.50 mol %). After 5 min, the individual reaction mixtures were transferred into rectangular molds to accomplish the second step of the reaction. The molds, 70 cm/80 cm/0.08 cm in dimension, were prepared using Teflon spacers along the three edges of a pair of glass plates. The open side along the remaining edge was partially closed by a smaller spacer, leaving two orifices at the corners. Nitrogen gas was purged through one of the orifices, while the other was used to inject the reaction mixture under gentle steam of nitrogen. The molds were then placed vertically in a thermostated water bath at 41 ± 1°C and dipped up to the height of reaction mixtures. Nitrogen purging was stopped after 10 min and the orifices were closed using paraffin grease. After 24 h of reaction, the transparent PADMA membranes were removed from the molds, cut into pieces, washed in regularly changed distilled water for 3 days to remove the unreacted monomers, and dried in vacuum. Feed composition of the five PADMA membranes, PADMA50–PADMA90, and corresponding synthesis parameters are listed in Table I.

In addition to the PADMA copolymers, homopolymers of AAc and DMAPMA (PAAc and PDMAPMA, respectively) were prepared to elucidate the molecular structure. Here, the reaction conditions were maintained similar to those of PADMA membranes with only difference lying in the second step, which was done in test tubes instead of rectangular molds. PAAc was obtained as a cylindrical solid, whereas, PDMAPMA was precipitated from 2-butanone after 24 h.

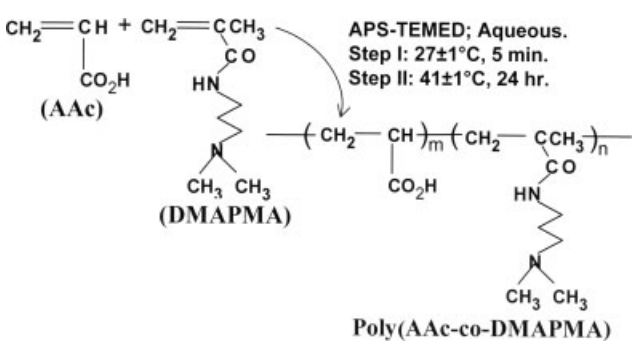

Scheme 1 Synthesis of poly(AAc-*co*-DMAPMA) hydrogel membranes (PADMAs).

TABLE I
Feed Composition of PADMA Membranes[a]

Sample code	AAc (mol %)	DMAPMA (mol %)	Water (mol %)[b]
PADMA50	50	50	326
PADMA72	72	28	276
PADMA80	80	20	253
PADMA86	86	14	233
PADMA90	90	10	217

[a] Concentration of APS and TEMED in feed was 0.5 mol % and 3.0 mol %, respectively.
[b] mol % to total monomer content.

FTIR analysis

The infrared experiments were performed using a Perkin–Elmer Spectrum One infrared spectrometer (ATR–FTIR). Samples were placed separately on the ZnSe crystal and the spectra were collected in the wave number range of 4000–650 cm^{-1}, at 4 cm^{-1} resolution.

Swelling experiment

To determine the equilibrium swelling *in vitro*, the dried PADMA discs were weighed and incubated in SBF at 37 ± 1°C. At equilibrium, the discs were removed from the solution and reweighed after careful removal of the excess surface water. The swelling ratio (Q) was then calculated as $(W_f - W_i)/W_i \times 100$, where W_f and W_i are the final weight of the swollen discs and the initial weight of the dry discs, respectively. Each experiment was performed in triplicate.

SEM analysis

Stereoscan 360 Scanning Electron Microscope (SEM) of Cambridge Scientific Industries was used to investigate the morphology of PADMA membranes, before and after swelling in simulated body fluid (SBF). All of the samples were lyophilized and kept in vacuum till silver sputtering treatment.

Optical microscopic analysis

Leitz Laborlux 12 Pol microscope, fitted with digital camera JVC, TIC-C1380E (A), was used to study the pore size of SBF-swollen PADMA membranes. The transparent membranes, equilibrated in SBF, were placed under the microscope and the images were recorded at a magnification of 10×. The diameter of the pores was calculated by Leica Qwin Software for optical microscopy.

Hemocompatibility

Hemocompatibility of PADMA membranes was evaluated through thrombogenicity assay and hemolysis assay. Corresponding experiments were carried out according to the methods described previously.[32,33]

Thrombogenicity assay

Thrombogenicity of PADMA membranes was evaluated using a whole blood kinetic clotting time method. Blood was drawn from a healthy adult volunteer by venipuncture and collected in vacutainer tubes containing trisodium citrate as the anti coagulant. Briefly, freshly prepared PADMA membranes were cut into pieces of 10 mm in diameter and washed thoroughly with regularly changed distilled water. Prior to the experiment, the discs were rinsed with normal saline and then placed in the wells of 12 well plates. The clotting reaction was activated with the addition of 1 mL $CaCl_2$ (0.1*M*) to 10 mL of the citrated blood. One Hundred microliter of the activated blood was carefully added to the PADMA membranes. All samples were incubated at 37 ± 1°C for 10, 20, 30, 40, and 50 min. The samples were further incubated with 3 mL of distilled water for 5 min at the end of each time point. The red blood cells that were not trapped in a thrombus were lysed with the addition of distilled water, thereby releasing hemoglobin into the water. All the aliquots were half diluted and the concentration of hemoglobin was measured by monitoring the absorbance at 545 nm in Perkin–Elmer Lambda EZ201 UV/VIS Spectrophotometer. Each experiment was done in triplicate. The absorbance values were plotted against the corresponding contacting times.

Hemolysis assay

Healthy human blood was collected in vacutainer tubes, as mentioned earlier. PADMA membranes were equilibrated with normal saline and were cut into pieces of 10 mm in diameter before being transferred into screw capped polystyrene tubes. Ten milliliter of normal saline was poured into each of the tubes and kept at 37°C in a shaking water bath. After 60 min incubation, 200 μL of diluted citrated blood (8 mL citrated blood was diluted with 10 mL normal saline) was dropped into each of the tubes. All of the tubes were further incubated at 37 ± 1°C for 60 min. Similarly, positive and negative controls were produced in separate tubes by adding 200 μL of the diluted blood to 10 mL of distilled water and normal saline, respectively. The fluids were then transferred into fresh polystyrene tubes and centrifuged at 5000 rpm for 15 min. Optical density of the

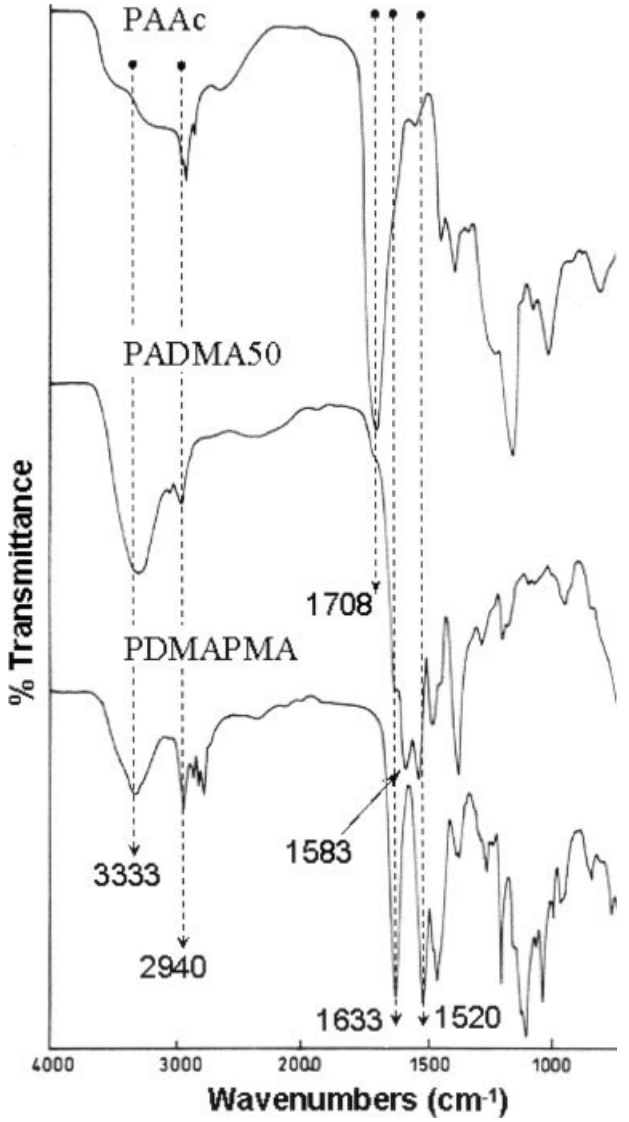

Figure 1 FTIR spectra of PAAc, PDMAPMA, and PADMA50. Important peaks in PADMA50, which are identical to that of any of the two homopolymers are marked by dotted arrows, passing vertically through the concerned peaks. Corresponding peak values are placed at the arrow heads. Important new peak found in PADMA50 is marked by a discrete arrow.

supernatants were measured at 545 nm. The hemolysis ratio (HR) was evaluated using the equation HR = 100 × (AS − AN)/(AP − AN), where AS, AP, and AN are the absorbance of sample supernatant, positive control, and negative control, respectively.

Diffusion study

Franz's diffusion cell, with an internal diameter of 3 cm, was used to evaluate the diffusion coefficient (D) of salicylic acid (SA) through the PADMA membranes. The donor and receptor chambers were separated by the PADMA membranes, which in turn were equilibrated in SBF prior to the experiments. Three hundred milligram of SA was dissolved in 5 mL of ethanol and the volume was made up to 100 mL by distilled water to make 0.3% (w/v) SA solution. Five milliliter of SA solution was taken in the donor chamber. The receptor chamber, equipped with a magnetic stir bar and a sampling port, contained 59 mL of distilled water. The receptor fluid was kept in constant stirring at 37°C during diffusion experiment. The temperature was maintained constant by circulating water through the jacket, surrounding the receptor chamber. 0.1 mL of donor aliquot was withdrawn and 1.0 mL of the receptor fluid was replaced by distilled water periodically at stipulated intervals of time. The concentration of SA in each chamber, as a function of time, was determined by spectrophotometric analysis of the withdrawn aliquots at 297 nm. Diffusion coefficient was subsequently calculated from these results, neglecting the minimal error associated with the gradual change in osmotic pressure due to the withdrawal of donor aliquot.

RESULTS AND DISCUSSION

FTIR characterization

FTIR spectra of PAAc, PDMAPMA, and PADMA50 membrane are shown in Figure 1.

Important peaks in PADMA50, identical to that of PAAc or PDMAPMA, are marked by vertically aligned dotted arrows. Important new peak found in PADMA50 is marked by a discrete arrow. Absorption bands at 3333, 1633, and 1520 cm^{-1} in PDMAPMA were assigned to N—H stretching, amide I, and amide II, respectively. The strong band at 1708 cm^{-1} was due to the stretching vibration of carboxyl carbonyl group (C=O of COOH) in PAAc.

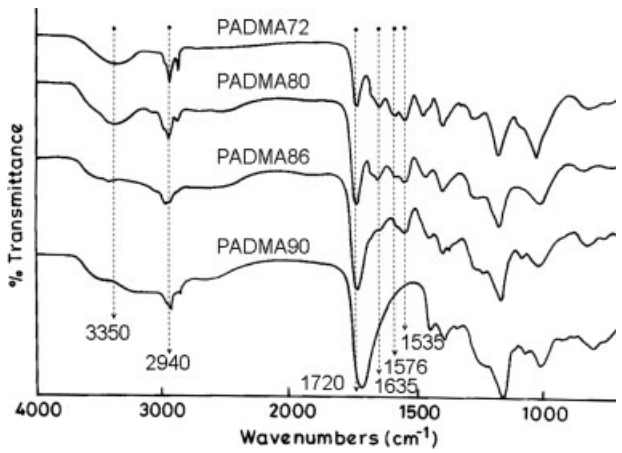

Figure 2 FTIR spectra of PADMA72, PADMA80, PADMA86, and PADMA90.

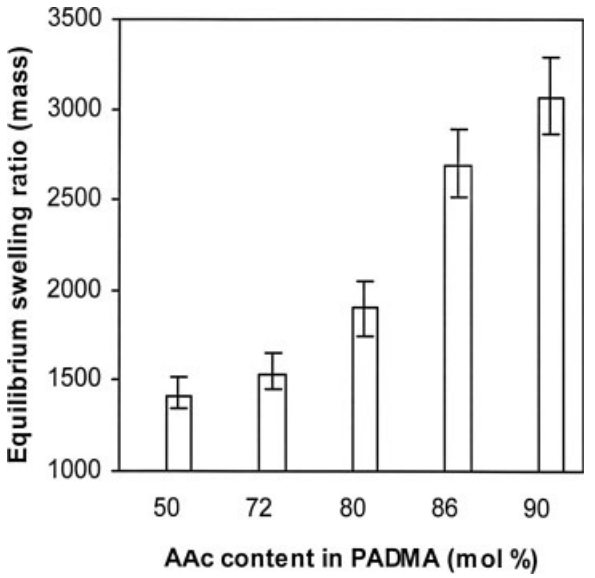

Figure 3 Equilibrium swelling of PADMA membranes in SBF at 37 ± 1°C.

Absorption at 2940 cm^{-1} was due to the C—H stretching. Presence of DMAPMA units in PADMA50 membrane is evident from the IR spectra. The strong band at 1708 cm^{-1} of PAAc reduced to a weak shoulder in PADMA50, and a new band appeared at 1583 cm^{-1}. This new band was due to the asymmetric stretching of carboxylate ions ($—COO^-$). Decrease of —COOH groups and appearance of $—COO^-$ ions was due to the ionic complex formation between AAc and DMAPMA units in PADMA50. FTIR spectra of other PADMA membranes are shown in Figure 2.

Equilibrium swelling in SBF

Equilibrium swelling ratios (Qs) of PADMA membranes in SBF at 37 ± 1°C are shown in Figure 3.

With composition, considerable variation was observed in the degree of swelling. PADMA50, having stoichiometric ratio of AAc and DMAPMA, undergoes the minimum swelling of 1412%. The swelling ratio increases with the increase of AAc content, reaches maximum in PADMA90 with a Q of 3066%. This is because of the fact that pKa of PAAc is ~ 4.75.[34] Most of the AAc units in PADMAs remain ionized at pH 7.4 and result in the ionic repulsion along the polymer chains. The extent of repulsion increases with AAc content in PADMAs, leading to the increase in swelling ratio. It is worthwhile to mention here that all of the PADMA membranes remain dimensionally stable in the swollen state.

SEM morphological observation

SEM images of PADMA membranes are shown in Figure 4. Surface morphology of PADMA90 before swelling is shown in Figure 4(A). The membrane was found to be composed of closely packed nanogels of ~ 200 nm in diameter. It is already mentioned that all PADMA membranes remain dimensionally stable when equilibrated in SBF. Three-dimensional network structures were expected and were verified by SEM. Figure 4(B) shows the surface morphology of SBF-swollen PADMA90. Macroporous mesh was seen at low magnification. It is worthwhile to remember here that the membranes were fabricated without using chemical crosslinker or radiation. The nanogels appeared as the building blocks of the matrices and were found to remain interconnected even after swelliing. Figure 4(C) shows the interconnected nanogels, as were observed in the SBF-swollen PADMA90. It is beyond the scope of this contribution to investigate the mechanism of the formation of these nanogels *in situ*. These interconnected nanogels might have some role in the dimensional stability of PADMA membranes.

Optical microscopic observation

Environmental scanning electron microscope is generally used to investigate the morphology of swollen hydrogels in wet condition. However, we have used

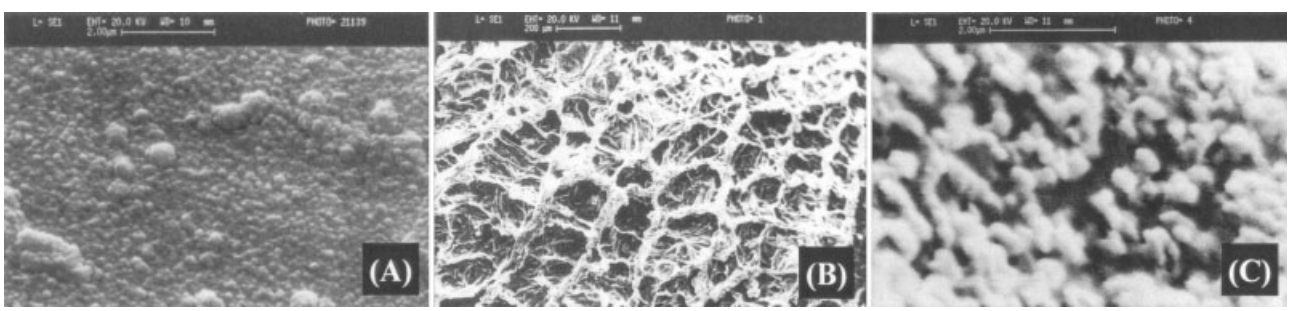

Figure 4 SEM micrographs of the surface of PADMA90: (A) before swelling; (B) after swelling, at low magnification; (C) after swelling, at high magnification.

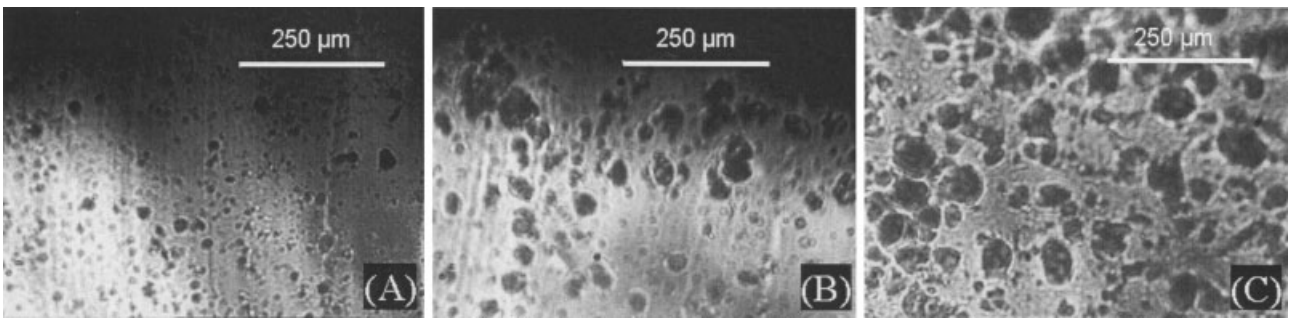

Figure 5 Optical micrographs of SBF-swollen PADMA membranes: (A) PADMA50, (B) PADMA80, (C) PADMA90 (magnification = 10×).

an optical microscope to investigate the variation of pore size with composition in SBF-swollen PADMAs. Images of PADMA50, PADMA80, and PADMA90, captured at a constant magnification of 10×, are shown in Figure 5(A–C), respectively.

In each case, diameter of 12 most prominent pores was measured. Arithmetic mean of those 12 readings was considered to be the average pore size. It was observed that the pore size of PADMA membranes increases with the increase in AAc content. The average pore size of PADMA50, PADMA80, and PAMA90 was 46, 72, and 94 μm, respectively (neglecting the decimal points). It is to be noted that manual error was not unlikely in the quantitative measurement of the average pore sizes. This was because of the complication that arises from the adjustment of focus at the pores of a particular sample. Not all of the visible pores, but only a fraction could be brought in focus. However, variation in pore size with the composition of PADMA membranes could be assessed at least qualitatively. Gradual increase in pore size through PADMA50–PADMA90 is evident from the images of Figure 5. This variation was due to the increase in equilibrium swelling with the increase in AAc content.

Thrombogenicity assay

Concentration of hemoglobin in the blood solution is inversely proportional to the size of blood clot. Therefore, higher absorbance values indicate improved thromboresistance of material. In the present thrombogenicity assay, the blood solutions obtained after 10, 20, 30, 40, and 50 min were diluted to half of its concentration and the corresponding absorbance values are shown in Figure 6.

Thrombus formation was found to decrease gradually with the increase of DMAPMA content in the membranes. Significant thromboresistivity was observed in PADMA50 and PADMA72.

Hemolysis assay

The extent of RBC rupture in blood, due to the contact of any material, is represented by hemolysis ratio (HR). Permissible limit of HR for acceptable biomaterials was reported to be 5%.[33] HR of PADMA membranes are shown in Table II.

PADMA90 was recorded to cause minimum hemolysis with a HR of 0.08%. Extent of hemolysis was observed to increase gradually from PADMA90 to PADMA50. However, the maximum hemolysis due to PADMA50 was only 1.66%, which is well under the permissible limit. Therefore, all the PADMA membranes could be considered to be highly hemocompatible and may be suitable as biomaterials for specific application purposes.

Diffusion coefficient

Typical variation of the amount of SA in the two chambers, when the receptor contained distilled water, during a single experiment with PADMA72 is shown in Figure 7.

It was observed that SA content gradually decreases in the donor chamber and simultaneously increases in the receptor. SA concentrations in the

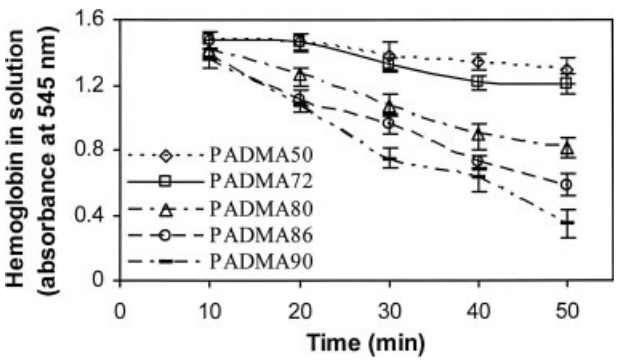

Figure 6 Effect of PADMA membranes on thrombus formation in human blood at 10, 20, 30, 40, and 50 min. Thrombus size is inversely proportional to the absorbance.

TABLE II
Effect of PADMA Membranes on Hemolysis Ratio (HR)

Sample	Optical density at 545 nm	HR (%)
Water	1.161	+ ve control
Saline	0.023	− ve control
PADMA50	0.042	1.66
PADMA72	0.031	0.70
PADMA80	0.028	0.43
PADMA86	0.027	0.35
PADMA90	0.024	0.08

two chambers at any time, t, could be used to calculate the diffusion coefficient (D) of SA through the membrane using the following equation [eq. (1)]:[35]

$$D = \frac{1}{\beta t} \times \ln \frac{C_D(t) - C_R(t)}{C_D(0) - C_R(0)} \quad (1)$$

with,

$$\beta = \frac{A_H}{W_H} \times \left[\frac{1}{V_1} + \frac{1}{V_2}\right]$$

where, $C_D(0)$ = initial concentration of SA in donor; $C_R(0)$ = initial concentration of SA in receptor; $C_D(t)$ = concentration of SA in donor after time t; $C_R(t)$ = concentration of SA in receptor after time t; A_H = effective cross sectional area of diffusion in the membrane; W_H = width of the membrane; V_1 = volume of SA solution; and V_2 = volume of distilled water in receptor.

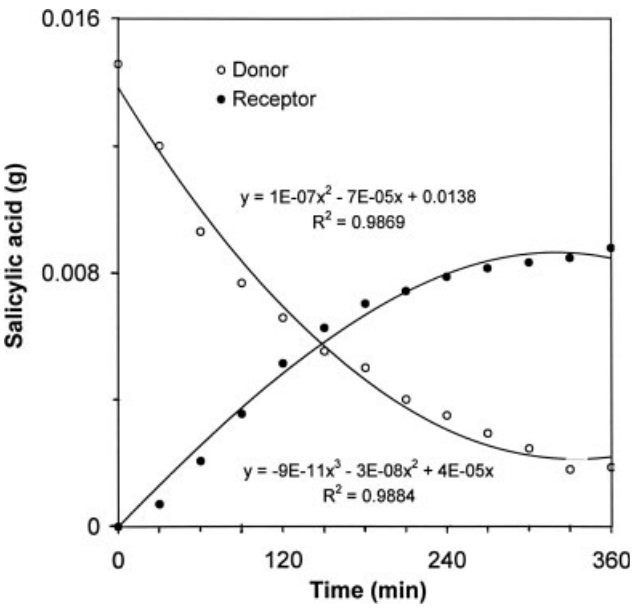

Figure 7 Variation of the amount of SA (grams) in the donor and receptor chambers of Franz's diffusion cell as a function of time during the diffusion experiment with PADMA72.

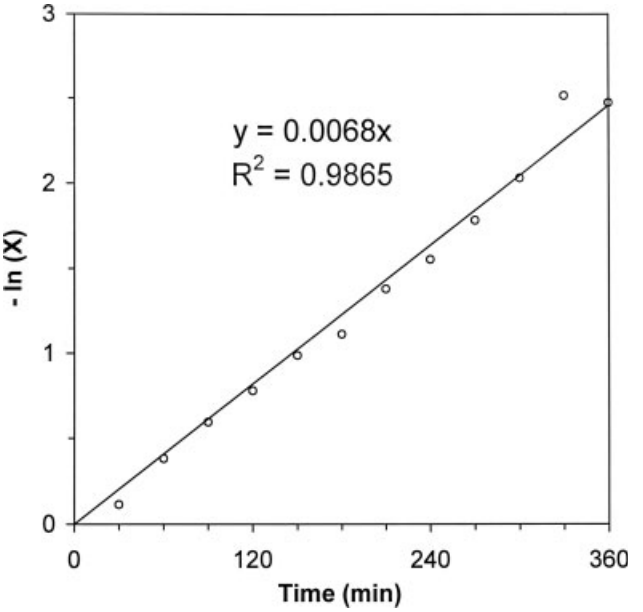

Figure 8 Variation of $-\ln X$ as a function of time in the diffusion of SA through PADMA72.

A plot of $-\ln \frac{C_D(t) - C_R(t)}{C_D(0) - C_R(0)}$ (denoted by –ln X) with time, as shown in Figure 8, yielded a straight line. The slope of this line can be used to calculate D. Diffusion coefficient of SA through PADMA72 was found to be 4.10×10^{-6} cm^2/s. Similarly, D of SA through PADMA90 was found to be 10.34×10^{-6} cm^2/s. This increase in D may be due to the increase in pore size.

CONCLUSIONS

A series of hydrogel membranes (PADMAs) were fabricated from AAc and DMAPMA, without using chemical crosslinker or radiation. Presence of the two monomer units and their electrolytic complexation in PADMA membranes were ensured by FTIR spectroscopy. Several *in vitro* experiments were carried out in SBF in order to mimic the behavior of PADMA membranes in physiological fluid. By varying the monomer feed composition, significant modulation was achieved in the properties associated with swelling. Degree of swelling as well as the pore size increases with the increase of AAc content in PADMA. All the PADMA membranes were found to be dimensionally stable in SBF. Significantly, morphological investigations revealed that the membranes were composed of closely packed nanogels of $\sim$ 200 nm. These interconnected nanogels were also observed in the macroporous network of swollen PADMA and might have some role in the remarkable dimensional stability of these physically crosslinked hydrogels. PADMA membranes were found to be hemocompatible with human blood and allow

diffusion of SA. Hence, these membranes could be tried for various biomedical applications, such as drug delivery systems and moist wound dressings.

References

1. Hoffman, A. S. Adv Drug Delivery Rev 2002, 54, 3.
2. Yoshida, R.; Sakai, K.; Okano, T.; Sakurai, Y. Adv Drug Delivery Rev 1993, 11, 85.
3. Nederberg, F.; Watanabe, J.; Ishihara, K.; Hilborn, J.; Bowden, T. Biomacromolecules 2005, 6, 3088.
4. Trank, S. J.; Johnson, D. W.; Cussler, E. L. Food Technol 1989, 43, 78.
5. Feil, H.; Bae, Y. H.; Kim, S. W. J Membr Sci 1991, 64, 283.
6. Park, T. G.; Hoffman, A. S. Enzyme Microb Technol 1993, 15, 476.
7. Shiroya, T.; Tamura, N.; Yasui, M.; Fujimoto, K.; Kawaguchi, H. Colloids Surf B 1995, 4, 267.
8. Chen, J. P.; Sun, Y. M.; Chu, D. H. Biotechnol Prog 1998, 14, 473.
9. Ogiso, M.; Minoura, N.; Shinbo, T.; Shimizu, T. Biomaterials 2006, 27, 4177.
10. Han, I. S.; Han, M. H.; Kim, J.; Lew, S.; Lee, Y. J.; Horkay, F.; Magda, J. J. Biomacromolecules 2002, 3, 1271.
11. Kajiwara, K.; Ross-Murphy, S. B. Nature 1992, 355, 208.
12. Osada, Y.; Okuzaki, H.; Hori, H. Nature 1992, 355, 242.
13. Ueoka, Y.; Gong, J.; Osada, Y. J. Intell Mater Syst Struct 1997, 8, 465.
14. Hennink, W. E.; van Nostrum, C. F. Adv Drug Delivery Rev 2002, 54, 13.
15. Boucard, N.; Viton, C.; Domard, A. Biomacromolecules 2005, 6, 3227.
16. Watanabe, T.; Ohtsuka, A.; Murase, N.; Barth, P.; Gersonde, K. Magn Reson Med 1996, 35, 697.
17. Qu, X.; Wirsen, A.; Albertson, A.-C. J Appl Polym Sci 1999, 74, 3186.
18. Wang, C.; Steward, R. J.; Kopecek, J. Nature 1999, 397, 417.
19. Torrado, S.; Prada, P.; Torre, P. M. de la; Torrado, S. Biomaterials 2004, 25, 917.
20. Zhao, Y.; Yang, Y.; Yang, X.; Xu, H. J Appl Polym Sci 2006, 102, 3857.
21. Park, K. Biomaterials 1988, 9, 435.
22. Ulbricht, M.; Riedel, M. Biomaterials 1998, 19, 1229.
23. Tanodekaew, S.; Prasitsilp, M.; Swasdison, S.; Thavornyutikarn, B.; Pothsree, T.; Pateepasen, R. Biomaterials 2004, 25, 1453.
24. Detomaso, L.; Gristina, R.; Sensei, G. S.; d'Agostino, R.; Favia, P. Biomaterials 2005, 26, 3831.
25. Wood, C.; Nguyen-Kim, S. UK Pat. WO 2003,084,484 (2003).
26. Peter, O. Beate, K. UK Pat. DE 19,921,895 (2000).
27. Çaykara, T.; Demiray, M.; Güven, O. Colloid Polym Sci 2005, 284, 258.
28. Tuncel, A.; Demirgoz, D.; Patir, S.; Piskin, E. J Appl Polym Sci 2002, 84, 2060.
29. Huang, J.-T.; Zhang, J.; Zhang, J.-Q.; Zheng, S.-H. J Appl Polym Sci 2005, 95, 358.
30. Bajpai, A. K.; Kankane, S. J Appl Polym Sci 2007, 104, 1559.
31. Kokubo, T.; Kushitani, H.; Sakka, S.; Kitsugi, T.; Yamamuro, T. J Biomed Mater Res 1990, 24, 721.
32. Motlagh, D.; Yang, J.; Lui, K. Y.; Webb, A. R.; Ameer, G. A. Biomaterials 2006, 27, 4315.
33. Shih, M. F.; Shau, M. D.; Chang, M. Y.; Chiou, S. K.; Chang, J. K.; Cherng, J. Y. Int J Pharm 2006, 327, 117.
34. Turan, E.; Çaykara, T. J Appl Polym Sci 2007, 106, 2000.
35. Cussler, E. L. Diffusional Mass Transfer in Fluid Systems, 2nd ed.; Cambridge University Press: New York, 1997; p 23.